Available online at www.sciencedirect.com
SCIENCE DIRECT
Biochimica et Biophysica Acta 1707 (2005) 179–188
BIOCHIMICA ET BIOPHYSICA ACTA
BBA
http://www.elsevier.com/locate/bba

The transient complex of poplar plastocyanin with cytochrome *f*: effects of ionic strength and pH

Christian Lange[a], Tobias Cornvik[a], Irene Díaz-Moreno[a,b], Marcellus Ubbink[a,*]

[a]*Leiden Institute of Chemistry, Leiden University, Gorlaeus Laboratories, P.O. Box 9502, 2300 RA Leiden, The Netherlands*
[b]*Instituto de Bioquímica Vegetal y Fotosíntesis, Universidad de Sevilla-CSIC. Avda. America Vespuccio, s/n. Seville 41092, Spain*

Received 19 August 2004; received in revised form 25 November 2004; accepted 1 December 2004
Available online 29 December 2004

Abstract

The orientation of poplar plastocyanin in the complex with turnip cytochrome *f* has been determined by rigid-body calculations using restraints from paramagnetic NMR measurements. The results show that poplar plastocyanin interacts with cytochrome *f* with the hydrophobic patch of plastocyanin close to the heme region on cytochrome *f* and via electrostatic interactions between the charged patches on both proteins. Plastocyanin is tilted relative to the orientation reported for spinach plastocyanin, resulting in a longer distance between iron and copper (13.9 Å). With increasing ionic strength, from 0.01 to 0.11 M, all observed chemical-shift changes decrease uniformly, supporting the idea that electrostatic forces contribute to complex formation. There is no indication for a rearrangement of the transient complex in this ionic strength range, contrary to what had been proposed earlier on the basis of kinetic data. By decreasing the pH from pH 7.7 to pH 5.5, the complex is destabilized. This may be attributed to the protonation of the conserved acidic patches or the copper ligand His87 in poplar plastocyanin, which are shown to have similar pK_a values. The results are interpreted in a two-step model for complex formation.

Keywords: Electron transfer; Photosynthesis; Protein complex; NMR spectroscopy; Transient complex

1. Introduction

Cytochrome *f* (Cyt *f*) is the electron exit port of the cytochrome b_6f complex, one of the membrane protein complexes involved in oxygenic photosynthesis [1]. It interacts transiently with the small electron transfer protein plastocyanin, which shuttles electrons from the cytochrome b_6f complex to Photosystem I. A proteolytic, water-soluble, fragment of Cyt *f* can be isolated from plant chloroplasts [2]. The crystal structure of the soluble fragment of Cyt *f* from turnip leaves (*Brassica rapa*) was the first to be determined [3]. The structure shows that Cyt *f* has an elongated shape with two domains consisting predominantly of β-sheets. The covalently bound heme group is buried in the larger domain close to the interface with the smaller domain (see Fig. 1). Surprisingly, the N-terminus of the protein acts as the sixth ligand to the heme iron, which is unique among *c*-type cytochromes. Cyt *f* from higher plants contains highly conserved basic residues, which take part in the interaction with Pc [4,5]. These residues, K58, K65, K66 in the large domain and K185, K187 and R209 in the small domain, form a basic ridge in Cyt *f* (see Fig. 1) suitable for the interaction with the acidic patches of Pc. The recent elucidation of two structures of the complete cytochrome b_6f complex [6,7] has demonstrated that Cyt *f* assumes a tilted orientation relative to the thylakoid membrane, with the heme area around ligand Tyr1 exposed to the lumen. Plastocyanin (Pc) is a protein of 10.5 kDa with a type-I copper site. The copper is coordinated by two histidine

Abbreviations: Cyt *f*, cytochrome *f*; ET, electron transfer; HSQC, heteronuclear single-quantum coherence spectroscopy; IPTG, isopropylthio-β-D-galactoside; NMR, nuclear magnetic resonance; NOESY, nuclear Overhauser effect spectroscopy; Pc, plastocyanin; PCS, pseudocontact shift(s); PMSF, phenylmethylsulfonylfluorid; TOCSY, total correlation spectroscopy; TSP, sodium 3-(trimethylsilyl)-2,2,3,3-d_4-propionate

* Corresponding author. Tel.: +31 71 527 4628; fax: +31 71 527 4349.
E-mail address: m.ubbink@chem.leidenuniv.nl (M. Ubbink).

0005-2728/$ - see front matter © 2004 Elsevier B.V. All rights reserved.
doi:10.1016/j.bbabio.2004.12.002

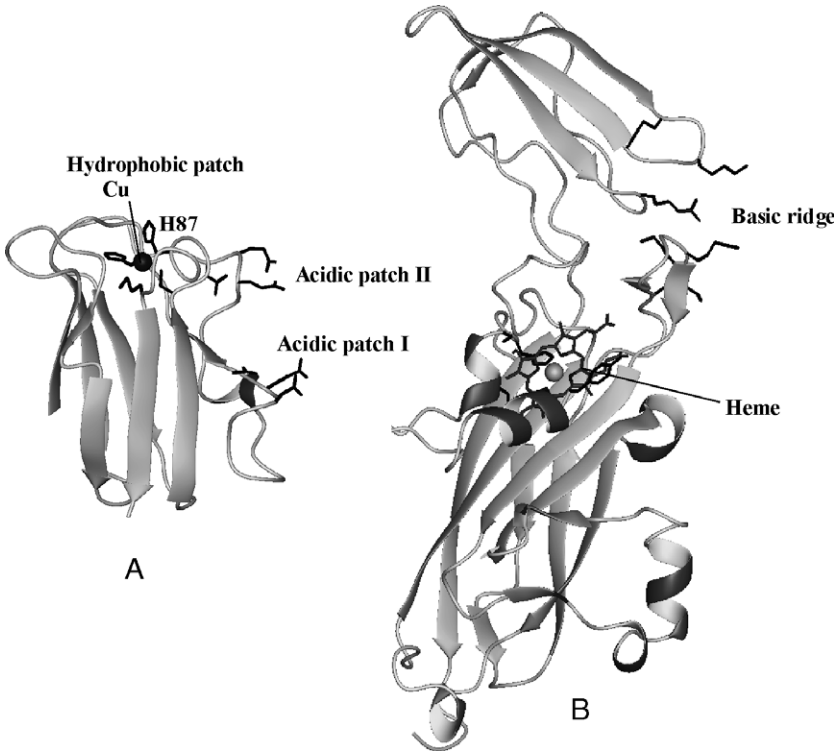

Fig. 1. Plastocyanin and cytochrome *f*. Ribbon representation of (A) poplar Pc (PDB entry 5PCY) with the copper center as a sphere and the copper ligands and acidic residues shown as black sticks and of (B) turnip Cyt *f* (PDB entry 1CTM) with the heme group, Y1 and some basic residues as black sticks. The figure was prepared with the program MOLMOL [44].

residues, one cysteine and one methionine residue (see Fig. 1). Poplar Pc was the first Pc to be crystallized and have its structure determined by X-ray crystallography [8–11]. The structure has shown that Pc contains eight β-strands forming two sheets. The copper site is buried below a relatively flat hydrophobic patch made up by residues in loop regions. Pcs from plants contain two highly conserved patches of negatively charged residues [12]. Acidic patch I comprises residues 42–45, whereas acidic patch II is formed by residues 59–61. These patches are located on one side of the protein with the acidic patch I located more remotely from the copper site than patch II. Based on chemical cross-linking [13] and site-directed mutagenesis [14,15] it has been proposed that the acidic patches are involved in the interaction of Pc with its partners.

The structure of the transient complex of spinach Pc and the water-soluble fragment of turnip Cyt *f* has been determined by NMR spectroscopy employing the paramagnetism of the heme [16]. The structure of the complex shows that spinach Pc binds to Cyt *f* with both its acidic patches and the hydrophobic patch involved. Residues in the acidic patches of Pc interact with residues of the basic patch of Cyt *f*. Furthermore, the close proximity of H87 with the heme of Cyt *f* suggests that H87 is the site of electron entry into Pc. The observed distance of 11 Å between the heme iron and the copper center allows for fast ET.

Numerous studies on the interaction of Pc with Cyt *f* from plants have shown that the kinetics of Pc reduction is slowed down by an increase of ionic strength (see Ref. [1] for a review). However, some studies indicated that there is an optimal ionic strength for the reduction of Pc by Cyt *f*, as seen from bell-shaped dependencies [17–19]. This has been explained by proposing that at very low ionic strength binding is dominated by electrostatic interactions resulting in a conformation that is less reactive. In line with this idea, Qin and Kostic [20] found evidence for the occurrence of a rearrangement step during the complex formation of Pc and Cyt *f*, because a cross-linked form of the complex was not active in ET.

For reduced poplar Pc it has been shown that the geometry of the copper site depends strongly on the pH due to protonation of the H87 imidazol group [10]. Kinetic measurements have shown that ET from Cyt *f* to Pc is influenced by the pH with an optimum around pH 7.5 [21]. It is unknown whether this pH dependence is related to the protonation of H87.

In the present work, the structure of the complex of poplar (*Populus nigra*) Pc and turnip (*B. rapa*) Cyt *f* has been determined by a rigid-body docking calculation using restraints from paramagnetic NMR measurements. Furthermore, the ionic strength and the pH dependence of the complex have been studied in order to clarify (a) whether the proposed rearrangement with ionic strength results in observable structural changes in the complex and (b) what the effect is of protonation of H87 on the complex of Pc and Cyt *f*.

2. Materials and methods

2.1. Protein preparation

^{15}N-labeled poplar Pc was expressed in the cytoplasm of *Escherichia coli* BL21 cells using plasmid pETPc [22]. Bacteria were cultured at 30 °C and 250 rpm to an OD_{600} of 0.8 in minimal medium as described [23] with the following changes. Sodium-sulfate was used instead of potassium-sulfate and no molybdenum salts were added. Per liter medium 5 g glucose and 0.5 g $^{15}NH_4Cl$ (~96% ^{15}N enrichment, Cambridge Isotopes Laboratories) were used. Ten milliliters of vitamin mixture [24] was added and yeast extract was omitted. Expression was induced by the addition of 0.4 mM IPTG and 100 μM copper citrate was added and incubation was continued for 4.5 h. Cells were harvested by centrifugation, resuspended in 20 mM sodium-phosphate buffer pH 7.0 with 1 mM PMSF and 100 μM copper chloride and were lysed using a French pressure cell. Cell debris was removed by centrifugation at 6000 rpm for 20 min and membranes were removed by ultracentrifugation at 35,000 rpm for 30 min. The protein was purified using a DEAE-fastflow sepharose (Amersham Biosciences) column under reducing conditions, followed by sephadex G-75 (Amersham Pharmacia Biotech) size-exclusion chromatography of the oxidized protein and finally elution from a DEAE-fastflow sepharose column of the oxidized protein. Protein purity was checked by SDS-PAGE and isoelectric focusing and by the ratio A_{280}/A_{597} of the oxidized protein (0.9). Pc concentrations were determined spectrophotometrically using the extinction coefficient ε_{597}=4700 $M^{-1}cm^{-1}$ [25] for oxidized Pc. The yield was 12 mg/L of culture.

The water-soluble fragment of turnip Cyt *f* was expressed in the periplasm of *E. coli* W3110 cells using plasmid pTC1, which contains the genes of the signal peptide of azurin from *Pseudomonas aeruginosa* and the fragment of turnip Cyt *f* including the first 252 residues. Two successive PCR steps were performed for the construction of plasmid pTC1. For amplification of the leader sequence of azurin from the *P. aeruginosa*, primer 1 (5′-GCTCACTCATTAGGCACCCCAGGC-3′) and primer 2 (5′-TTCATAATTCTGCTGGGCAAAAATTGGA-TAAGCCAGCAGCGGCGCACTGAG-3′) were used with plasmid pCD4, containing the azurin leader sequence, as template. The PCR product was then used as a megaprimer with primer 3 (5′-CCGAAGCTTCTATTGGACACG-TAATGGATCTTG-3′) and plasmid pUFMY containing the turnip Cyt *f* gene (kindly provided by Prof. J.C. Gray, Cambridge, UK). The resulting PCR product, cut with *Eco*RI and *Hin*dIII was cloned into pUC18 using the same restriction enzymes to give plasmid pTC1.

Cells were grown under semi-anaerobic conditions in 1.7 L of Luria-Bertani (LB) medium in 2 L Erlenmeyer flasks at 150 rpm at 30 °C for 68 h. The medium was supplemented with 1 mM KNO_3, 4 mM sodium-fumarate and 100 μg/mL ampicillin. After harvesting the cells by centrifugation periplasmic proteins were released using an osmotic shock treatment [26]. The periplasmic fraction was loaded onto a DEAE-fastflow sepharose column and the Cyt *f* was eluted with 300 mM NaCl. The protein was then purified further using the protocol described by Gong et al. [5]. The protein purity was checked by SDS-PAGE and isoelectric focusing. The concentration of reduced Cyt *f* was determined spectrophotometrically using the extinction coefficient of ε_{554}=31500 $M^{-1}cm^{-1}$ [16].

Cadmium substituted Pc was prepared as described before [27].

2.2. NMR experiments

All NMR spectra were obtained at 303 K using a Bruker DMX600 spectrometer. [^{15}N, ^{1}H-]-HSQC-TOCSY and [^{15}N, ^{1}H-]-HSQC-NOESY spectra with mixing times of 56 ms and 100 ms respectively were acquired for verification of the assignments.

To measure pseudocontact shifts (PCS), a [^{15}N, ^{1}H-]-HSQC spectrum [28] was acquired of a solution of 0.5 mM Cd-substituted ^{15}N-labelled Pc and 0.35 mM oxidized turnip Cyt *f* in 10 mM sodium phosphate pH 6.0. Then, Cyt *f* was reduced by the addition of a slight excess of sodium ascorbate, the pH was readjusted to 6.0 and another HSQC spectrum was acquired. The difference of the chemical shifts for Pc amides in the presence of oxidized Cyt *f* and those observed with reduced Cyt *f* gives the PCS.

The effect of ionic strength on complex formation was measured with an NMR sample containing 0.10 mM of reduced poplar Pc and 0.06 mM of reduced turnip Cyt *f* in 10 mM sodium-phosphate buffer, pH 6.0, with 1 mM sodium-ascorbate, 6% (v:v) D_2O and 100 μM TSP. The ionic strength was adjusted by adding NaCl from a 1 M stock solution to the NMR sample. Control spectra were recorded under the same conditions with 0.15 mM free Pc.

For measurement of the pH dependence of complex formation a sample of 0.1 mM reduced poplar Pc and 0.04 mM reduced turnip Cyt *f* was used in 5 mM sodium-acetate, 5 mM sodium-phosphate and 5 mM Tris/HCl, pH 8.0. The pH was adjusted by adding HCl from a 0.1 M stock solution. The pH was measured before and after each experiment and averaged. The maximum pH change during the NMR experiment was 0.05 pH units for free Pc and 0.1 pH units for Pc with Cyt *f*. To determine the chemical-shift perturbations of binding, the chemical shifts of Pc in the complex were compared with those of free Pc at the same pH.

2.3. Data processing and analysis

Data processing was performed using AZARA (available from www.bio.cam.ac.uk/azara). The ^{1}H- and ^{15}N-resonance assignments for poplar Pc were taken from BioMagResBank

(accession code 4019, Koide, S., Gippert, G., Reymond, M. and Wright, P.E., unpublished data). Chemical-shift perturbations of ^{15}N and ^{1}H nuclei for Pc upon interaction with Cyt *f* were analyzed by overlaying the spectra of bound Pc with the free protein in the assignment program ANSIG [29]. Line widths of NMR signals were measured using the software XWINNMR from Bruker.

Titration curves were fitted with the equation $\delta=(K_{a*}H+[H^+]*L)/(K_a+[H^+])$ using the software ORIGIN version 5.0 (Microcal), with H and L being the chemical-shift values at infinitely high and low pH, respectively.

2.4. Structure calculation

Structure calculations were performed using XPLOR-NIH version 2.9.1 [30,31]. The structures of poplar Pc (PDB entry 5PCY, [11]) and turnip Cyt *f* (PDB entry 1HCZ, [32]) were treated as rigid bodies, and the coordinates of Cyt *f* were fixed. Pc was placed at a random position and allowed to move in a restrained rigid-body molecular dynamics calculation. None of the standard energy terms was used. Instead, several classes of experimental restraints were applied to dock the proteins.

I) Distance restraints were defined between 50 uniformly distributed backbone and side chain amide nitrogens of Pc and all backbone amide nitrogens of Cyt *f*, using the r^{-6} averaging option. These restraints could only be violated if Pc approached Cyt *f* too closely, and thus served as a weak van der Waals term to prevent extensive collisions.

II) For the amide nitrogens and protons of residues that showed chemical-shift perturbations of ≥0.1 and 0.03 ppm, respectively, under the conditions mentioned under the description of the NMR experiment, distance restraints were defined to all backbone amide nitrogens (r^{-6} averaging) of Cyt *f*, in order to assure contact between the corresponding Pc residues and the surface of Cyt *f* (interface restraints).

III) PCS were used to define distance restraints between the shifted amide proton or nitrogen nuclei and the iron in the heme in Cyt *f*. PCS ($\Delta\delta_{PCS}$) were calculated and evaluated iteratively as described in [16], using an occupancy factor F=0.25.

IV) If a PCS is positive, the nucleus-heme iron–Tyr 1N angle (θ) must be smaller than 54°, while for negative PCS, θ must be larger. On this basis, angle restraints were used for all nuclei exhibiting a PCS, as described before [16].

V) Amide groups of which neither proton nor nitrogen showed significant PCS were restrained to a minimal distance from the heme iron. This distance was set in an iterative fashion, similar to the restraints in group III.

VI) In some runs (see Results), electrostatic distance restraints were applied. The amide nitrogens of Pc residues E43, D44, E59 and E60 were restrained to be close to any of the Cyt *f* residues K58, K65, K66, K181, K185, K187, R184 or R209, under the assumption that these residues of Pc exhibit electrostatic interactions with the positive ridge on Cyt *f* [18,33].

Table S1 (Appendix A) lists the numbers and relative scaling factors for all groups of restraints. Table S2 (Appendix A) gives all the chemical-shift perturbations used in the calculations. Four thousand cycles of calculations were performed (7 h on a dual processor Pentium IV PC running under LINUX). Only structures with a total restraint 'energy' below a threshold (40 A.U.) were saved, yielding about 100 structures. To assure sufficient sampling of the orientation space, a large random displacement of Pc occurred when a (local) minimum had been found, as judged from a total restrained energy that had not changed for more 50% during ten cycles. About 200 of such displacements occurred in a representative run.

The resulting structures were ranked according total restraints energy and the top ten structures, with total restraint energy values from 30 from 34 (A.U.), were subjected to restrained energy minimization using the XPLOR-NIH repulsive van der Waals term with reduced scaling. The ten best structure models have been deposited in the Protein Data Bank under entry 1TKW.

3. Results

3.1. Expression of turnip Cyt f

In previous NMR studies the soluble fragment of Cyt *f* prepared from plant leaves has been used [16]. Here, the water-soluble fragment of turnip Cyt *f* has been expressed in the periplasm of *E. coli* W3110 cells using the plasmid pTC1. The yield of the expression was found to be rather poor with 0.2 mg Cyt *f* per liter culture. This is in contrast to the expression yield observed for the water-soluble fragment of Cyt *f* from *Phormidium laminosum* expressed in *E. coli* [34]. In that case, the use of plasmid pEC86 containing the cytochrome *c* maturation cassette from *E. coli* [35] significantly improved the yield (up to 15 mg/L). In the case of turnip Cyt *f*, however, cotransformation of pEC86 resulted in the appearance of an additional nonnative cytochrome species as judged by the optical spectrum and this species copurified with Cyt *f*. No increase in the yield of the native Cyt *f* was observed (results not shown). With the plasmid used, pTC1, heterologous Cyt *f* is translocated using the signal peptide of the bacterial blue copper protein azurin. This signal sequence is very efficient in the translocation of azurin toward the periplasmic space of *E. coli*. Also a construct of the turnip Cyt *f* gene with the signal sequence of *P. laminosum* Pc, which transfers *P. laminosum* Cyt *f* effectively, was unable to increase the yield of turnip Cyt *f* in *E. coli*.

3.2. Assignment of NMR signals

The ^{1}H and ^{15}N backbone and side chain resonance assignments of reduced poplar Pc at pH 7.0, 303 K were taken from BioMagResBank (acc. code 4019) to assign the signals of reduced poplar Pc at pH 6.0. [^{15}N,^{1}H-]-HSQC-TOCSY and [^{15}N,^{1}H-]-HSQC-NOESY spectra were used to verify the assignments.

For 33 out of the 98 assigned amides double signals were observed in the HSQC spectra. Mass spectrometry of the recombinant poplar Pc showed two signals, at 10,599 Da and 10,731 Da. Since the calculated value for ^{15}N-labeled poplar Pc is m=10600 Da, it can be assumed that the recombinant poplar Pc is only partly processed in the bacterial cytoplasm. Thus, double signals for residues 17–31, which are located in the vicinity of the N-terminus, and residues 69–76, which are located in an adjacent strand [9], were attributed to the presence of the N-terminal methionine in a fraction of the protein.

3.3. Mapping of the binding interface by chemical-shift perturbation

Upon the addition of reduced Cyt *f* to ^{15}N labeled Pc(Cu I) at an ionic strength of 11 mM some of the signals in the [^{15}N,^{1}H-]-HSQC spectrum experience a change in their chemical-shift values (Table S3 in Appendix A). The formation of the complex of Pc and Cyt *f* is also evident from an increase in line width by about 8 Hz compared to the line width of free Pc. Assuming a binding constant of 22 mM^{-1} at this ionic strength, as found for pea Pc and turnip Cyt *f* (Ubbink, M., unpublished data), about one third of all Pc is bound under these experimental conditions.

Sixteen residues show chemical-shift changes of more than 0.1 ppm for ^{15}N nuclei. Effects are observed in the hydrophobic patch (residues S11, A13, F35, H37, V40, L62, L63 H87, Q88 and A90-M92), as well as in the acidic patches (D44-I46 in patch I and E59 in patch II).

For ^{1}H resonances, 27 residues in total show chemical-shift changes of more than 0.02 ppm. Most chemical-shift changes were found for residues in the first loop of Pc (G6–F14), most pronounced for residues S11 and L12. Also, residues N31, A33–F35, H37, A52, L62, K66, G67 and residues of the so-called ligand-loop (C84–M92) show changes in their chemical shifts. Residues in the acidic patch I (D42–S45) show large changes in their ^{1}H chemical shift whereas residues in the acidic patch II show only minor changes in their ^{1}H chemical shift.

In the [^{15}N,^{1}H-]-HSQC spectra signals for the side chains of N31, N32, N38, N64, N76, Q88 and N99 can be observed. In the presence of Cyt *f* the side chain signals of N31, N32, N38, N64 and Q88 are shifted, but not those of N76 and N99 (results not shown). In summary, the largest chemical-shift changes observed are located in the first loop and the ligand loop of Pc. Intermediate chemical-shift changes are located in the acidic patch I whereas the acidic patch II only shows small chemical-shift changes.

3.4. Orientation of Pc in the complex with Cyt *f*

The orientation of Pc relative to Cyt *f* in the complex was determined as described before [16]. The copper in Pc was replaced with the redox-inactive substitute cadmium, the amides were assigned (Table S4 in Appendix A) and the chemical-shift perturbations of amide groups of Pc(Cd) with either oxidized or reduced Cyt *f* were determined. With the reduced form, the Pc perturbations represent the effects of binding, as described above for Pc(Cu I). With oxidized Cyt *f*, amide groups in Pc experience additional intermolecular pseudocontact shifts (PCS) caused by the paramagnetic nature of the Fe(III) in the heme (Fig. S1 in Appendix A).

The binding effects and the PCS can be used to determine the orientation of Pc relative to Cyt *f* in the complex. Both types of shifts are translated into restraints for a rigid-body docking calculation. The binding shifts are used in a qualitative manner: Any shift larger than the threshold yields a restraint that requires that the amide is brought close to the surface of Cyt *f*. The PCS are used quantitatively: During the calculations, the PCS are calculated for the given position of Pc and compared with the experimental values. If the difference is larger than the error margins, the restraint is violated. The position of Pc is changed and the PCS are calculated again. Thus, in an iterative fashion, the optimal position with minimal restraint violations is found [16]. The calculations were performed in two ways. In the first run, only binding restraints and PCS restraints were included. In the second, also electrostatic restraints were introduced (see Materials and methods).

In the absence of electrostatic restraints two clusters of orientations are found. All high-ranking structures are part of cluster A, with Pc in a side-on orientation, allowing both the acid patches and the hydrophobic patch to make contact with the surface of Cyt *f*. In cluster B, Pc makes contact with Cyt *f* via the copper ligand loop only and has a longer average Fe–Cu distance (13.9 and 16.5 Å for clusters A and B, respectively) and no short electron transfer pathway is present. Cluster B yields an imbalanced distribution of violations, with many for the interface restraints and almost none for the pseudocontact restraints. It is concluded that cluster A represents the true complex, while B is a non-physical solution, because it is optimized neither in electrostatic interactions nor in electron transfer rate. In the presence of electrostatic restraints, only cluster A is observed. The average RMSD relative to the mean of the position of Pc in complex with Cyt *f* is reduced considerably to 2.2 Å, yielding a much better defined orientation of Pc in the complex than is obtained in the absence of the electrostatic restraints. The ten best

Fig. 2. The structure of the complex of poplar Pc and turnip Cyt *f*. The ten best orientations for Pc are shown as C^{α} traces (gray). The position of spinach Pc (PDB entry 2PCF, model 6) is shown as a black C^{α} trace. Cyt *f* is represented as a ribbon model. The heme is shown in sticks and the iron and coppers are shown as spheres.

structures of the run with electrostatic restraints are shown in Fig. 2 in light gray.

In these structures, the acidic patches are in contact with the positive ridge of Cyt *f* and the hydrophobic region is in close contact with the region around the heme group. The Fe–Cu distance is 13.9±0.7 Å. The largest binding shifts were observed for the residues His87, Ala90 and Gly91 and this region is in the center of the interface. Also the loop including Leu12 and the region around Asp44 are in contact with Cyt *f*. Only the region around Gly34 is not in contact with Cyt *f*, resulting in some violations of the interface restraints from this region. A violation analysis of the PCS and the angle restraints is provided in Fig. S2 (Appendix A).

3.5. Ionic strength dependence of the Pc–Cyt f interaction

To investigate the effect of the ionic strength on complex formation, [^{15}N, ^{1}H-]-HSQC spectra of Pc(Cu I) with reduced Cyt *f* were recorded at ionic strengths of 11, 21, 31, 41, 61 and 111 mM. Reference spectra were taken with free Pc under the same conditions. The effect of the ionic strength on the transient complex is evident from observing the line widths of residues Pc in the complex. With increasing ionic strength the line widths decrease and at 111 mM reach the value measured for free Pc (see Fig. 3A). This can be interpreted as destabilization of the complex by the ionic strength and is clear evidence for electrostatic interactions contributing to the interactions of Pc with Cyt *f*.

The observed chemical-shift changes for residues in Pc have been mapped onto the surface of the crystal structure of Pc for the different ionic strengths (see Fig. S3 in Appendix A). With increasing ionic strength, all of the observed chemical-shift changes decrease uniformly in the hydrophobic patch and the acidic patches, confirming that the complex is weakened by increasing the ionic strength. From the chemical-shift mapping no differences in the ionic strength dependence of the chemical-shift changes can be observed for residues in the hydrophobic patch and the acidic patches, which is confirmed by a plot of the relative chemical-shift changes (see Fig. 3B). These results suggest that the observed binding effects represent a single orientation of Pc in the complex, and not a dynamic average

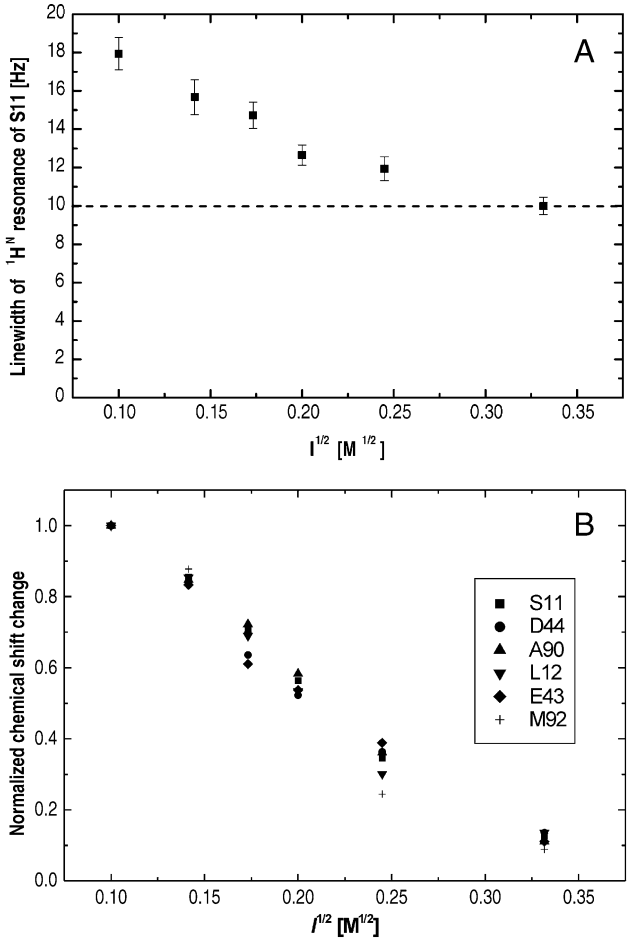

Fig. 3. Effect of ionic strength on complex formation. (A) Line width at half-height for S11 of Pc at different ionic strength values of a solution containing Pc (100 μM) and Cyt *f* (60 μM). The dashed line indicates the line width of S11 observed with free Pc. (B) Chemical-shift changes $\Delta\delta_{Bind}$ for residues in Pc at different ionic strength values, normalized against the value at *I*=11 mM.

of several well-defined complexes. As will be discussed later, this does not exclude the existence of a dynamic ensemble of many orientations.

3.6. pH dependence of the Pc–Cyt *f* interaction

One of the most remarkable findings of the X-ray structures of poplar Pc was that the geometry of the copper site of reduced poplar Pc, but not of oxidized Pc, strongly depends on the pH. This has been attributed to the protonation of H87 and its dissociation from the copper center. It has been suggested that this process acts as a molecular switch for photosynthetic ET involving Pc [10]. To study the effect of the protonation of H87 on complex formation with Cyt *f* a pH titration has been performed both for free Pc (from pH 7.7 to 4.7) and for the Pc–Cyt *f* complex (from pH 7.7 to 5.3).

In free Pc, resonances showing the most pronounced changes in their ^{15}N chemical shift during the pH titration are those of H37, N38, I39, D44, H87, Q88 and M92. The titration curves of H37, N38, H87, Q88 and M92 can be fitted with a global pK_a value of 4.95 (±0.02) (see Fig. 4). The titration curves for residues D42, E43, D44, E59, E60 and D61 can be fitted with pK_a values of 4.5, 5.3, 5.0, 4.7, 5.1 and 4.7, respectively (not shown). The pK_a values of residues G6, N31, A33, H37, N38, H87 and M92 are ascribed to the titration of the H87 side chain, an indication that this titration significantly affects either the structure or the charge distribution of the copper site in Pc.

The effect of pH on the interaction of Pc with Cyt *f* can be seen from the chemical-shift changes observed in the pH range from 7.7 to 5.5 (see Fig. 5). All shifts decrease with decreasing pH to ca. 60% of their magnitude at pH 7.7. The decrease is only small above pH 6 and more drastic below pH 6, suggesting a decrease in the affinity below this pH. The total ionic strength was 20.5 mM and varied less than 10% over the pH range, as a consequence of compensation effects of the three buffers used. Thus, effects due to ionic strength variations can be excluded. The variation between residues of the chemical-shift changes with pH is greater than in the case of the ionic strength titration. This could indicate a rearrangement of the complex interface with decreasing pH, as was observed also in the complex of *P. laminosum* [34].

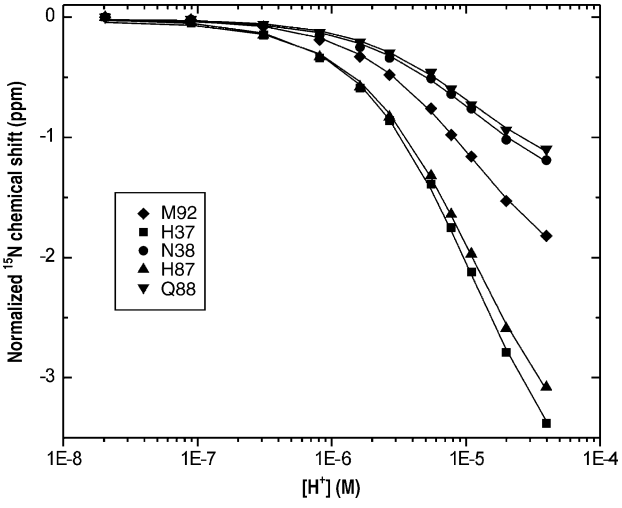

Fig. 4. pH effects on free Pc. Titration curves based on ^{15}N chemical shifts for amides that show a pK_a=4.95±0.02, attributed to the titration of the His87 side chain. Shifts are normalized relative to the shift at pH 7.7.

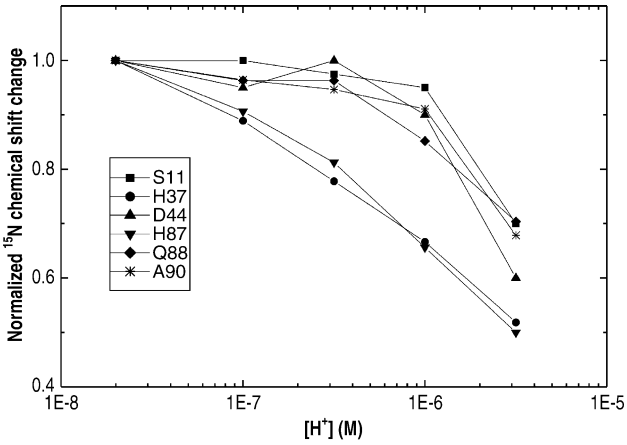

Fig. 5. pH effect on the complex of Pc and Cyt *f*. Chemical-shift changes of amide ^{15}N resonances of several Pc residues in the Pc–Cyt *f* complex as a function of pH from pH 7.7 to 5.5. Shifts are normalized relative to the shift at pH 7.7. The lines are shown to guide the eye.

4. Discussion

4.1. The structure of the complex

The orientation of Pc in the complex could be determined using a combination of binding site information and pseudocontact restraints. Similar to the orientation of Pc in the only other structurally characterized plant complex, of turnip Cyt *f* and spinach Pc, the hydrophobic patch of poplar Pc is located close to the heme region, while extensive electrostatic interactions occur between the acidic patches of Pc and the basic ridge of Cyt *f*. However, the complexes are significantly different. In the complex with poplar Pc, the plastocyanin is tilted with regard to the position of spinach Pc (see Fig. 2, with spinach Pc shown as a black C^{α}-trace), bringing the copper ligand loop very close to the heme region and preventing further approach of the His87 side chain towards the heme. Consequently, the Fe–Cu distance is larger for the complex with poplar Pc, compared to that with spinach Pc, 13.9 and 10.9 Å, respectively. Also, the distance between the Cyt *f* Tyr 1 heme ligand and Pc His87 copper ligand is larger (3.5±0.6 Å for the Tyr C^{ϵ}–His $C^{\delta 2}$ distance in the poplar complex, 2.9 Å for the Tyr $C^{\delta 2}$–His $N^{\epsilon 2}$ distance in spinach). However, the residues are still sufficiently close for rapid ET. In several of the models

shorter distances are observed for other atoms, e.g. between the Cyt *f* Tyr 1 O^{η} and the carbonyl O of Pro 86 in Pc. These contacts could also facilitate ET.

On the basis of the NMR chemical-shift perturbations and docking simulations, it has been suggested that also parsley Pc is slightly tilted compared to spinach Pc, in a direction however, that is opposite of that for poplar. In that model the Fe–Cu distance is 13.0 Å [36].

In the current study the occupancy factor was 0.25 (0.20 was used in the structure with spinach). The occupancy factor is a scaling term (see Eq. (4) in [16]) for the fraction of time that Pc experiences the PCS. Pc is in fast exchange between bound and free states and, thus, the observed chemical shifts are an average between both states. From the binding constant, it can be estimated that 57% Pc was in the bound state in this experiment. The fact that the occupancy factor is smaller than 0.57 could indicate that the scalar value of the axial term of the magnetic susceptibility tensor, which was derived from EPR data, is smaller than estimated. Alternatively, the low occupancy factor could indicate that within the complex, Pc is not in the well-defined orientation close to the heme all the time, but, instead, is partly in a dynamic state that does not yield PCS. This view is in agreement with the model of protein complex formation, in which a dynamic state precedes the formation of a well-defined complex [[37], vide infra].

The effect of including electrostatic restraints in the calculation of the orientation of Pc in the complex was analyzed. Such restraints are not based on NMR data, but on kinetic data, which showed that electrostatic forces contribute to the affinity of binding [18,33]. In the absence of the electrostatic restraints, the same orientation of Pc is found, but with a larger spread in the various orientations. Thus, the electrostatic restraints improve the precision of the structure of the complex.

In view of the recent structures of the cytochrome b_6f complex [6,7], the binding site for Pc on Cyt *f* described here appears to be readily accessible in the full complex. Fig. 6 shows a model of the complex Pc and cytochrome b_6f obtained after the alignment of the Cyts *f* of the structure determined here and the crystal structure of the cytochrome b_6f complex from *Chlamydomonas reinhardtii* [7].

Fig. 6. Model of the complex of Pc and cytochrome b_6f. The model was obtained after alignment of the Cyts *f* of the complex of poplar Pc and turnip Cyt *f* (present work) and the crystal structure of the cytochrome b_6f from *C. reinhardtii* (PDB entry 1Q90) [7]. The cytochrome b_6f is shown in ribbons, except the Rieske protein, which is shown as a C^{α} trace. Pc is shown at the top, also as a C^{α} trace. The figure was generated using Diepview and rendered with PovRay.

4.2. Ionic strength dependence of Pc–Cyt f interaction

The data demonstrate that the interactions in the Pc–Cyt *f* complex from plants are affected by the ionic strength. With increasing ionic strength all the observed chemical-shift changes decrease. Also, the line widths of the resonances of Pc in the complex show a decrease with increasing the ionic strength. This can be attributed to a weakening of the complex when the ionic strength increases and is further evidence that the Pc–Cyt *f* complex from higher plants is stabilized by electrostatic forces. In contrast to this finding, the affinity of Pc and Cyt *f* from the thermophilic cyanobacterium *P. laminosum* is hardly affected by changes in the ionic strength [34].

Previously, it has been shown by laser flash [17] and stopped-flow [18] experiments that the kinetics of Pc reduction by Cyt *f* exhibits a bell-shaped ionic strength dependence, with the maximal rate being achieved around 30 mM. It has been suggested that below the optimal ionic strength non-productive complexes are formed, which can be reoriented by an increase in ionic strength to yield the complex with optimal ET kinetics.

Our NMR data indicate that, within experimental error, the binding shifts of all residues decrease equally with increasing ionic strength, between 11 mM and 111 mM. The uniform behavior of the shifted peaks with changing ionic strength indicates that there is no large rearrangement from one well-defined orientation to another.

A more realistic picture is that of two-step complex formation, in which a highly dynamic ensemble of orienta-

tions (collectively called the encounter complex) precedes the formation of the active, single orientation complex. As we discussed before [16], such a state, which is maintained primarily by electrostatic interactions, results in only very small chemical shift changes [38,39], which would be masked by the large chemical-shift changes of the single orientation complex, and thus remain invisible in our NMR experiments. On the basis of kinetic data Hart et al. [40] recently used the following scheme to describe the reaction between Pc and Cyt *f*:

$$\mathrm{Pc_{ox}} + \mathrm{Cyt}f_{\mathrm{red}} \underset{k_{-a}}{\overset{k_a}{\rightleftarrows}} [\mathrm{Pc_{ox}{:}Cyt}f_{\mathrm{red}}] \underset{k_{-r}}{\overset{k_r}{\rightleftarrows}} [\mathrm{Pc_{ox}Cyt}f_{\mathrm{red}}] \underset{k_{-et}}{\overset{k_{et}}{\rightleftarrows}} [\mathrm{Pc_{red}Cyt}f_{\mathrm{ox}}]$$

In this scheme, [Pc_{ox}:Cyt f_{red}] and [Pc_{ox}Cyt f_{red}] represent the encounter complex and the active complex, respectively. The former is invisible in our NMR experiments and only the latter is observed. Hart et al. show that the binding constant $K_A=K_aK_r$, with $K_a=k_a/k_{-a}$ and $K_r=k_r/k_{-r}$. With increasing ionic strength, K_a decreases monotonically due to electrostatic screening, shifting leftmost equilibrium to the left. However, K_r may increase, because the encounter complex is purely electrostatic, while the single orientation complex also involves hydrophobic interactions. This would shift the middle equilibrium to the right. The change in K_r represents the shift from the non-reactive toward reactive form that was invoked to explain the bell-shaped kinetics. This implies that the amount of single-orientation complex, [Pc_{ox}Cyt f_{red}], decreases somewhat more slowly than expected from the fraction of bound protein. Careful comparison of the two panels in Fig. 3 lends some support to this interpretation: The line width, which is directly proportional to the total fraction of bound Pc, [Pc_{ox}:Cyt f_{red}]+[Pc_{ox}Cyt f_{red}], decreases more rapidly than the binding shifts, which are proportional to [Pc_{ox}Cyt f_{red}] only, suggesting a shift of the middle equilibrium to the right. Thus, the two step complex formation model with a highly dynamic encounter complex is able to reconcile the bell-shaped kinetics and the NMR results. Similarly, it helped to explain the different ionic strength behavior of the Pc and Cyt *f* complex of *P. laminosum* as observed with kinetic measurements and NMR experiments [40]. The dynamic, specific nature of the electrostatic interactions is also in accord with the finding that the precise location of the acidic patches is not very relevant [41].

4.3. pH dependence of Pc–Cyt f interaction

Many amides surrounding the copper experience a pK_a of 4.95, which is ascribed to the protonation of H87. Clearly, this protonation has significant effects on the environment of the copper site. This has also been observed for Pc from *P. laminosum* [34]. The pK_a value for H87 is in the range of other plant Pcs [42]. However, the value found in this study is considerably larger than a pK_a value of 4.6 found for poplar Pc by UV resonance Raman spectroscopy [43].

The binding shifts of Pc in the complex are also sensitive to pH. The non-uniform changes for various residues suggest reorganization in the complex with decreasing pH. Below pH 6, a general decrease of the shifts suggests a decrease in the affinity, which is supported by a reduction of the line widths (results not shown). This finding is in agreement with a decrease in the reduction rate of Pc by Cyt *f* at low pH [21]. In the case of the Pc:Cyt *f* complex from *P. laminosum*, there is no evidence that protonation of the copper ligand H92 affects the affinity [34]. In the plant complex, the protonation of homologous Pc residue H87 has a pK_a similar to that of the acidic residues in patches I and II, so in the case of the plant proteins it remains to be established which titratable groups are responsible for the decrease in the affinity.

Acknowledgements

CL and IDM acknowledge financial support of the Program Human Potential and Mobility of Researchers of the European Commission (contract no. HPRN-CT-1999-00095, ‘Transient Network’) and the Spanish Ministry of Education, Culture and Sport (AP2000-2937). MU is supported financially by the Netherlands Organisation for Scientific Research (grant 700.52.425).

Appendix A. Supplementary Data

Supplementary data associated with this article can be found, in the online version, at doi:10.1016/j.bbabio.2004.12.002.

References

[1] A.B. Hope, Electron transfers amongst cytochrome *f*, plastocyanin and Photosystem I: kinetics and mechanisms, Biochim. Biophys. Acta 1456 (2000) 5–26.
[2] J.C. Gray, Purification and properties of monomeric cytochrome *f* from charlock, *Sinapis arvensis* L, Eur. J. Biochem. 82 (1978) 133–141.
[3] S.E. Martinez, D. Huang, A. Szczepaniak, W.A. Cramer, J.L. Smith, Crystal structure of chloroplast cytochrome *f* reveals a novel cytochrome fold and unexpected haem ligation, Structure 2 (1994) 95–105.
[4] G.M. Soriano, M.V. Ponamarev, R.A. Piskorowski, W.A. Cramer, Identification of the basic residues of cytochrome *f* responsible for electrostatic docking interactions with plastocyanin in vitro: relevance to the electron transfer reaction in vivo, Biochemistry 37 (1998) 15120–15128.
[5] X.S. Gong, J.Q. Wen, J.C. Gray, The role of amino-acid residues in the hydrophobic patch surrounding the haem group of cytochrome *f* in the interaction with plastocyanin, Eur. J. Biochem. 267 (2000) 1732–1742.
[6] G. Kurisu, H.M. Zhang, J.L. Smith, W.A. Cramer, Structure of the cytochrome b_6f complex of oxygenic photosynthesis: tuning the cavity, Science 302 (2003) 1009–1014.
[7] D. Stroebel, Y. Choquet, J.L. Popot, D. Picot, An atypical haem in the cytochrome b_6f complex, Nature 426 (2003) 413–418.

[8] P.M. Colman, H.C. Freeman, J.M. Guss, M. Murata, V.A. Norris, J.A.M. Ramshaw, M.P. Venkatappa, X-ray crystal structure analysis of plastocyanin at 2.7 Å resolution, Nature 272 (1978) 319–324.
[9] J.M. Guss, H.C. Freeman, Structure of oxidized poplar plastocyanin at 1.6 Å resolution, J. Mol. Biol. 169 (1983) 521–563.
[10] J.M. Guss, P.R. Harrowell, M. Murata, V.A. Norris, H.C. Freeman, Crystal structure analyses of reduced (CuI) poplar plastocyanin at six pH values, J. Mol. Biol. 192 (1986) 361–387.
[11] J.M. Guss, H.D. Bartunik, H.C. Freeman, Accuracy and precision in protein structure analysis: restrained least-squares refinement of the structure of poplar plastocyanin at 1.33 Å resolution, Acta Crystallogr., B 48 (1992) 790–811.
[12] M.R. Redinbo, T.O. Yeates, S. Merchant, Plastocyanin: structural and functional analysis, J. Bioenerg. Biomembranes 26 (1994) 49–66.
[13] L.Z. Morand, M.K. Frame, K.K. Colvert, D.A. Johnson, D.W. Krogmann, D.J. Davis, Plastocyanin cytochrome *f* interaction, Biochemistry 28 (1989) 8039–8047.
[14] S. Young, K. Sigfridsson, K. Olesen, O. Hansson, The involvement of the two acidic patches of spinach plastocyanin in the reaction with Photosystem I, Biochim. Biophys. Acta 1322 (1997) 106–114.
[15] J. Illerhaus, L. Altschmied, J. Reichert, E. Zak, R.G. Herrmann, W. Haehnel, Dynamic interaction of plastocyanin with the cytochrome *bf* complex, J. Biol. Chem. 275 (2000) 17590–17595.
[16] M. Ubbink, M. Ejdebäck, B.G. Karlsson, D.S. Bendall, The structure of the complex of plastocyanin and cytochrome *f*, determined by paramagnetic NMR and restrained rigid-body molecular dynamics, Structure 6 (1998) 323–335.
[17] T.E. Meyer, Z.G. Zhao, M.A. Cusanovich, G. Tollin, Transient kinetics of electron transfer from a variety of *c*-type cytochrome to plastocyanin, Biochemistry 32 (1993) 4552–4559.
[18] A. Kannt, S. Young, D.S. Bendall, The role of acidic residues of plastocyanin in its interaction with cytochrome *f*, Biochim. Biophys. Acta 1277 (1996) 115–126.
[19] B.G. Schlarb-Ridley, D.S. Bendall, C.J. Howe, Role of electrostatics in the interaction between cytochrome *f* and plastocyanin of the cyanobacterium *Phormidium laminosum*, Biochemistry 41 (2002) 3279–3285.
[20] L. Qin, N.M. Kostić, Importance of protein rearrangement in the electron-transfer between the physiological partners cytochrome *f* and plastocyanin, Biochemistry 32 (1993) 6073–6080.
[21] A.B. Hope, D.B. Mathews, P. Valente, Effects of pH on the kinetics of reactions in and around the cytochrome *bf* complex in an isolated system, Photosynth. Res. 42 (1994) 111–120.
[22] J.A. Ybe, M.H. Hecht, Periplasmic fractionation of *Escherichia coli* yields recombinant plastocyanin despite the absence of a signal sequence, Protein Expr. Purif. 5 (1994) 317–323.
[23] M. Cai, Y. Huang, K. Sakaguchi, G.M. Clore, A.M. Gronenborn, R. Craigie, An efficient and cost-effective isotope labeling protocol for proteins expressed in *Escherichia coli*, J. Biomol. NMR 11 (1998) 97–102.
[24] R.A. Venters, C.C. Huang, I.B.T. Farmer, R. Troland, L.D. Spicer, C.A. Fierke, High-level $^{2}H/^{13}C/^{15}N$ labeling of proteins for NMR studies, J. Biomol. NMR 5 (1995) 339–344.
[25] S. Modi, M. Nordling, L.G. Lundberg, Ö. Hansson, D.S. Bendall, Reactivity of cytochromes *c* and *f* with mutant forms of spinach plastocyanin, Biochim. Biophys. Acta 1102 (1992) 85–90.
[26] H.C. Neu, L.A. Heppel, The release of enzymes from *Escherichia coli* by osmotic shock and during the formation of speroplasts, J. Biol. Chem. 240 (1965) 3685–3692.
[27] M. Ubbink, L.Y. Lian, S. Modi, P.A. Evans, D.S. Bendall, Analysis of the ^{1}H-NMR chemical shifts of Cu(I)-, Cu(II)- and Cd-substituted pea plastocyanin. metal-dependent differences in the hydrogen-bond network around the copper site, Eur. J. Biochem. 242 (1996) 132–147.
[28] P. Andersson, B. Gsell, B. Wipf, H. Senn, G. Otting, HMQC and HSQC experiments with water flip-back optimized for large proteins, J. Biomol. NMR 11 (1998) 279–288.
[29] P.J. Kraulis, ANSIG: a program for the assignment of protein proton two-dimensional NMR spectra by interactive computer graphics, J. Magn. Reson. 84 (1989) 627–633.
[30] A.T. Brunger, X-PLOR 3.1 manual, Yale University Press, Yale, 1992.
[31] C.D. Schwieters, J.J. Kuszewski, N. Tjandra, G.M. Clore, The XPLOR-NIH NMR molecular structure determination package, J. Magn. Res. 160 (2003) 65–73.
[32] S.E. Martinez, D. Huang, M. Ponomarev, W.A. Cramer, J.L. Smith, The heme redox center of chloroplast cytochrome *f* is linked to a buried five-water chain, Protein Sci. 5 (1996) 1081–1092.
[33] X.S. Gong, J.Q. Wen, N.E. Fisher, S. Young, C.J. Howe, D.S. Bendall, J.C. Gray, The role of individual lysine residues in the basic patch on turnip cytochrome *f* for electrostatic interactions with plastocyanin in vitro, Eur. J. Biochem. 267 (2000) 3461–3468.
[34] P.B. Crowley, G. Otting, B.G. Schlarb-Ridley, G.W. Canters, M. Ubbink, Hydrophobic interactions in a cyanobacterial plastocyanin–cytochrome *f* complex, J. Am. Chem. Soc. 123 (2001) 10444–10453.
[35] E. Arslan, H. Schulz, R. Zufferey, P. Kunzler, L. Thony-Meyer, Overproduction of the *Bradyrhizobium japonicum c*-type cytochrome subunits of the cbb_3 oxidase in Escherichia coli, Biochem. Biophys. Res. Commun. 251 (1998) 744–747.
[36] P.B. Crowley, D.M. Hunter, K. Sato, W. McFarlane, C. Dennison, The parsley plastocyanin-turnip cytochrome *f* complex: a structurally distorted but kinetically functional acidic patch, Biochem. J. 378 (2004) 45–51.
[37] P.B. Crowley, M. Ubbink, Close encounters of the transient kind: protein interactions in the photosynthetic redox chain investigated by NMR spectroscopy, Acc. Chem. Res. 36 (2003) 723–730.
[38] J.A. Worrall, Y. Liu, P.B. Crowley, J.M. Nocek, B.M. Hoffman, M. Ubbink, Myoglobin and cytochrome b_5: a nuclear magnetic resonance study of a highly dynamic protein complex, Biochemistry 41 (2002) 11721–11730.
[39] J.A. Worrall, W. Reinle, R. Bernhardt, M. Ubbink, Transient protein interactions studied by NMR spectroscopy: the case of cytochrome *c* and adrenodoxin, Biochemistry 42 (2003) 7068–7076.
[40] S.E. Hart, B.G. Schlarb-Ridley, C. Delon, D.S. Bendall, C. Howe, Role of charges on cytochrome *f* from the cyanobacterium *Phormidium laminosum* and its interaction with plastocyanin, Biochemistry 42 (2003) 4829–4836.
[41] K. Sato, T. Kohzuma, C. Dennison, Pseudospecificity of the acidic patch of plastocyanin for the interaction with cytochrome *f*, J. Am. Chem. Soc. 126 (2004) 3028–3029.
[42] J.D. Sinclair-Day, M.J. Sisley, A.G. Sykes, G.C. King, P.E. Wright, Acid dissociation constants for plastocyanin in the copper(I) state, J. Chem. Soc., Chem. Commun. 8 (1985) 505–507.
[43] Q. Wu, F. Li, W. Wang, M.H. Hecht, T.G. Spiro, UV Raman monitoring of histidine protonation and $H–^{2}H$ exchange in plastocyanin, J. Inorg. Biochem. 88 (2002) 381–387.
[44] R. Koradi, M. Billeter, K. Wüthrich, MOLMOL: a program for display and analysis of macromolecular structures, J. Mol. Graph. 14 (1996) 51–55.